From EMI to KNP-EMI: spectral properties and scalable solvers

Pietro Benedusi, Ada J. Ellingsrud, Halvor Herlyng,
Stefano Serra-Capizzano, Marie Rognes

MICROCARD workshop, Strasbourg
July 2023

The emerging EMI framework use a geometrically explicit representation of the cellular domains

Find the intracellular and extracellular potentials $\phi_i = \phi_i(x, t)$ and $\phi_e = \phi_e(x, t)$, and the transmembrane current $I_M = I_M(x.t)$ s.t.:

$$-\nabla \cdot (\sigma_i \nabla \phi_i) = 0 \qquad \text{in } \Omega_i, \qquad (1)$$

$$-\nabla \cdot (\sigma_e \nabla \phi_e) = 0 \qquad \text{in } \Omega_e, \qquad (2)$$

$$\phi_M = \phi_i - \phi_e \qquad \text{at } \Gamma, \qquad (3)$$

$$\sigma_e \nabla \phi_e \cdot n_e = -\sigma_i \nabla \phi_i \cdot n_i = I_M \qquad \text{at } \Gamma, \qquad (4)$$

$$\frac{\partial \phi_M}{\partial t} = \frac{1}{C_M}(I_M - I_{\text{ion}}) \qquad \text{at } \Gamma. \qquad (5)$$

Ion concentrations are assumed to be constant in space and time – often an accurate approximation, but not always . . .

[Krassowska & Neu 1994],
[Ying & Henriquez 2007],
[Tveito et al. 2017]

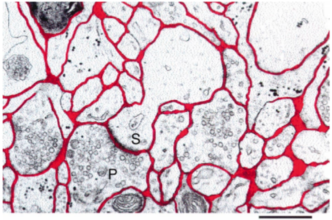

Rat cortex with ECS in red [Nicholson, 1998]

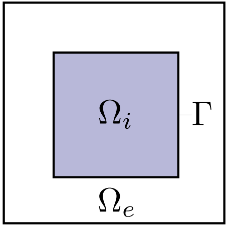

Encode the physiological role of complex geometries in 3D

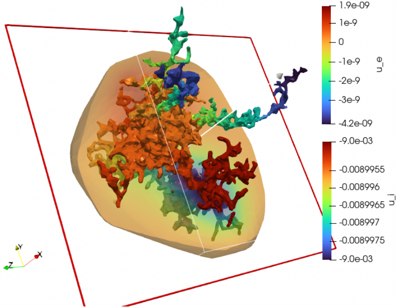

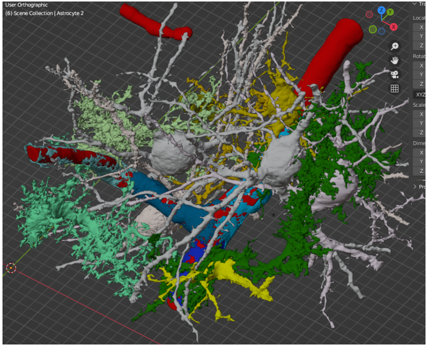

EMI formulations

Single-dimensional form

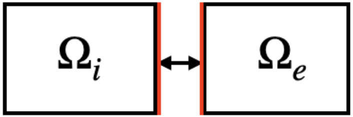

$$\begin{bmatrix} -\Delta_i & T_{ie} \\ T_{ie}' & -\Delta_e \end{bmatrix} \begin{bmatrix} \phi_i \\ \phi_e \end{bmatrix} = \begin{bmatrix} f_i \\ f_e \end{bmatrix}$$

CG+AMG

Multi-dimensional form

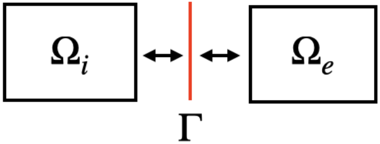

$$\begin{bmatrix} -\Delta_i & 0 & T_i \\ 0 & -\Delta_e & T_e \\ T_i' & T_e' & -I \end{bmatrix} \begin{bmatrix} \phi_i \\ \phi_e \\ I_m \end{bmatrix} = \begin{bmatrix} 0 \\ 0 \\ f \end{bmatrix}$$

GMRES+ILU

(singular blocks)

EMI Single-dimensional formulation

$$\begin{bmatrix} -\Delta_e & T_{ei} \\ T'_{ei} & -\Delta_i \end{bmatrix} \begin{bmatrix} \phi_e \\ \phi_i \end{bmatrix} = \begin{bmatrix} f_e \\ f_i \end{bmatrix}$$

more extensively:

$$\begin{bmatrix} CA_e^{\mathrm{in}} & CA_e^{\mathrm{in},\Gamma} & 0 & 0 \\ CA_e^{\Gamma,\mathrm{in}} & CA_e^{\Gamma} + M_e^{\Gamma} & 0 & T_{ei}^{\Gamma} \\ 0 & 0 & CA_i^{\mathrm{in}} & CA_i^{\mathrm{in},\Gamma} \\ 0 & (T_{ei}^{\Gamma})^T & CA_i^{\Gamma,\mathrm{in}} & CA_i^{\Gamma} + M_i^{\Gamma} \end{bmatrix} \begin{bmatrix} \phi_{\mathrm{in},e} \\ \phi_{\Gamma,e} \\ \phi_{\mathrm{in},i} \\ \phi_{\Gamma,i} \end{bmatrix} = \begin{bmatrix} \mathbf{0} \\ f_{\Gamma,e} \\ \mathbf{0} \\ f_{\Gamma,i} \end{bmatrix},$$

EMI Single-dimensional formulation: spectral properties

Theorem:
Assume that

$$N_\Gamma = o(\min\{N_i, N_e\}) \qquad \text{for} \quad N_\Gamma, N_i, N_e \to \infty,$$
$$\lim_{N_i, N_e \to \infty} \frac{N_i}{N_e + N_i} = r \in (0, 1)$$

then:

$$\begin{bmatrix} 0 & CA_e^{\mathrm{in},\Gamma} & 0 & 0 \\ CA_e^{\Gamma,\mathrm{in}} & CA_e^{\Gamma} + M_e^{\Gamma} & 0 & T_{ei}^{\Gamma} \\ 0 & 0 & 0 & CA_i^{\mathrm{in},\Gamma} \\ 0 & (T_{ei}^{\Gamma})^T & CA_i^{\Gamma,\mathrm{in}} & CA_i^{\Gamma} + M_i^{\Gamma} \end{bmatrix} \sim_\lambda 0.$$

Single-dimensional formulation: spectral properties

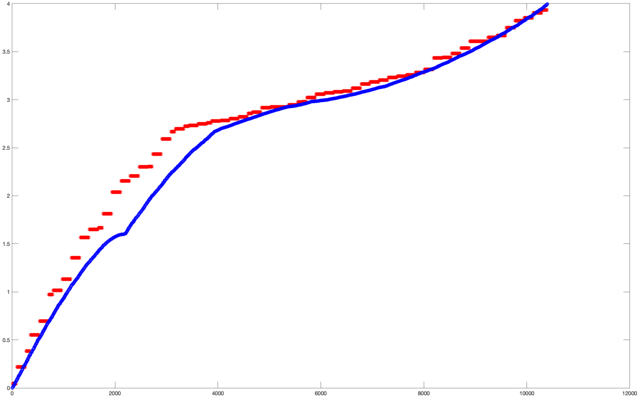

Numerical results: implementation

- CG(p)+CG(p)
- IMEX time stepping
- Fully parallel

- FEniCS and FEniCSx (+multiphenics)
- PETSc for solvers

```
# ASSEMBLE #
a11 = dt * inner(sigma_i*grad(ui), grad(vi))*dx(1) + C_M * inner(ui('-'), vi('-'))*dS
a22 = dt * inner(sigma_e*grad(ue), grad(ve))*dx(2) + C_M * inner(ue('+'), ve('+'))*dS
a12 = - C_M * inner(ue('+'), vi('-'))*dS
a21 = - C_M * inner(ui('-'), ve('+'))*dS

a = [[a11, a12],
     [ a21, a22]]
```

EMI: computational results

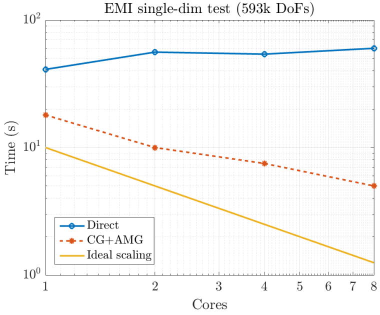

- Robust w.r.t. (n, p)
- Robust w.r.t. MPI procs
- Robust w.r.t. Δt

Δt	10^{-8}	10^{-7}	10^{-6}	10^{-5}	10^{-4}	10^{-3}	10^{-1}	10^{-2}	1
Iterations	5	6	5	5	5	5	5	5	5

- Robust w.r.t. geometry
- Robust w.r.t. dimensionality

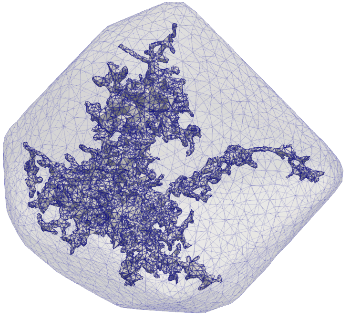

212k DoFs

MPI size	1	2	4	8
Iterations	5	5	5	5
Solve (s)	12.3	5.6	3.3	2.1

EMI: computational results

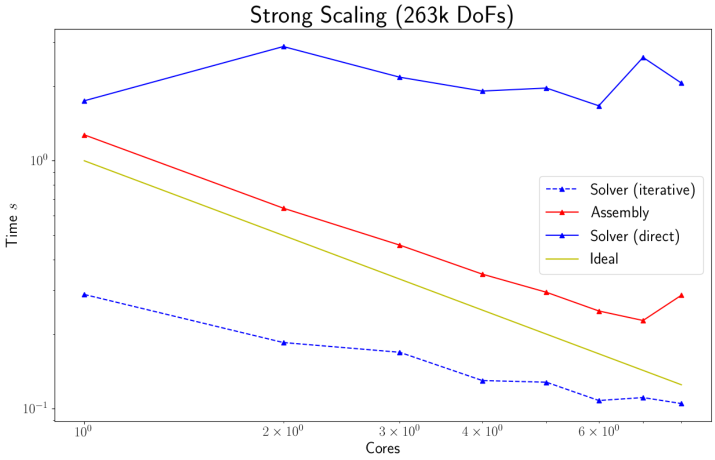

EMI: computational results

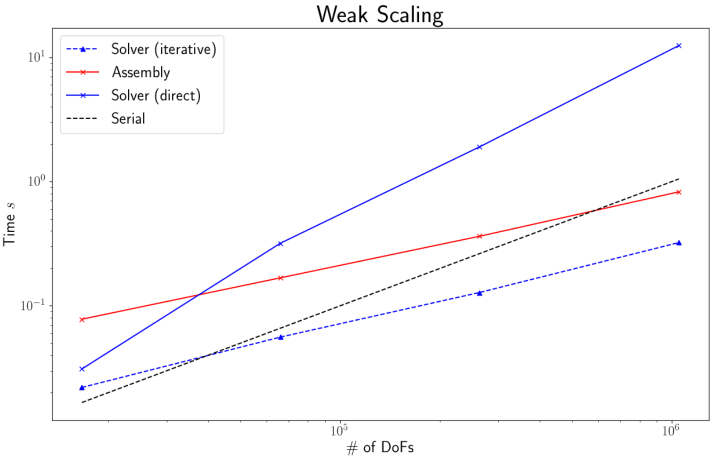

Movement of ions is fundamental in brain signalling, and ion concentration shifts are a trademark of several pathologies

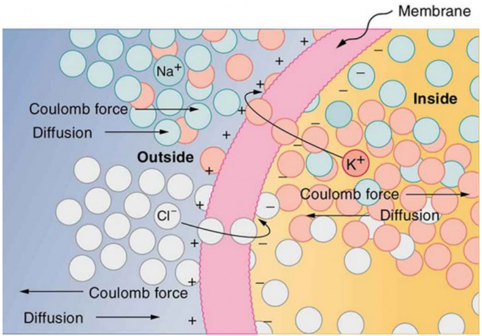

[courses.lumenlearning.com]

The extracellular ion composition changes with local neuronal activity and across brain states

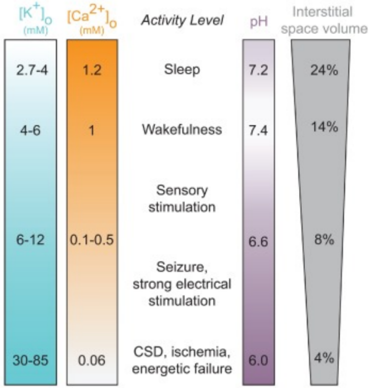

[Rasmussen, 2021]

A computational framework for ionic electrodiffusion in brain tissue with explicit representation of the cells (KNP-EMI)

For each ion species $k \in K$, find the *ion concentrations* $c_r^k : \Omega_r \times (0, T] \to \mathbb{R}$ and the *electrical potentials* $\phi_r : \Omega_r \times (0, T] \to \mathbb{R}$ such that:

$$\frac{\partial c_r^k}{\partial t} + \nabla \cdot \mathrm{J}_r^k = 0 \qquad \text{in } \Omega_r, \tag{6}$$

$$F \sum_k z^k \, \nabla \cdot \mathrm{J}_r^k = 0 \qquad \text{in } \Omega_r, \tag{7}$$

for $r = \{i, e\}$, where the ion flux densities are given by:

$$\mathrm{J}_r^k = -D_r^k \nabla c_r^k - D_r^k z^k \psi^{-1} c_r^k \nabla \phi_r, \qquad \text{in } \Omega_r. \tag{8}$$

The system remains to be closed by appropriate initial conditions, boundary conditions, and importantly interface conditions.

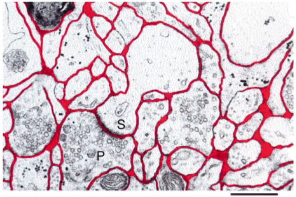

Rat cortex with ECS in red [Nicholson, 1998]

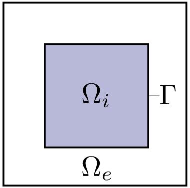

The KNP-EMI model: algebraic prospective

- IMEX linearization
- CG(p) + CG(p) discretization

Linear system on Ω_r

$$
\mathcal{A}_r = \left[\begin{array}{cccc|c}
M_r^1 + \tau_r^1 A_r^1 & 0 & \cdots & 0 & C_r^1 M_{r,\Gamma}^1 + \tilde{\tau}_r^1 \tilde{A}_r^1 \\
0 & M_r^2 + \tau_r^2 A_r^2 & 0 & \vdots & C_r^2 M_{r,\Gamma}^2 + \tilde{\tau}_r^2 \tilde{A}_r^2 \\
\vdots & 0 & \ddots & 0 & \vdots \\
0 & \cdots & 0 & M_r^{|K|} + \tau_r^{|K|} A_r^{|K|} & C_r^{|K|} M_{r,\Gamma}^{|K|} + \tilde{\tau}_r^{|K|} \tilde{A}_r^{|K|} \\
\hline
z^1 \tau_r^1 \tilde{A}_r^1 & z^2 \tau_r^2 \tilde{A}_r^2 & \cdots & z^{|K|} \tau_r^{|K|} \tilde{A}_r^{|K|} & C_m F^{-1} M_{r,\Gamma} + \tilde{\tau}_r A_r
\end{array}\right],
$$

The KNP-EMI model: algebraic prospective

$$\begin{bmatrix} \mathcal{A}_i^{cc} & \mathcal{A}_i^{c\phi} & 0 & \mathcal{T}_{ie}^{c\phi} & 0 \\ \mathcal{A}_i^{\phi c} & \mathcal{A}_i^{\phi\phi} & 0 & \mathcal{T}_{ie}^{\phi\phi} & 0 \\ 0 & \mathcal{T}_{ei}^{c\phi} & \mathcal{A}_e^{cc} & \mathcal{A}_e^{c\phi} & 0 \\ 0 & \mathcal{T}_{ei}^{\phi\phi} & \mathcal{A}_e^{\phi c} & \mathcal{A}_e^{\phi\phi} & w_e \\ 0 & 0 & 0 & w_e^T & 0 \end{bmatrix} \begin{bmatrix} c_i \\ \phi_i \\ c_e \\ \phi_e \\ \lambda_e \end{bmatrix} = \begin{bmatrix} f_i^c \\ f_i^\phi \\ f_e^c \\ f_e^\phi \\ 0 \end{bmatrix}$$

Given the regularization $\epsilon > 0$ coefficient,

$$\mathcal{P}(\epsilon) = \begin{bmatrix} \mathcal{A}_i^{cc} & 0 & 0 & 0 & 0 \\ 0 & \epsilon\mathcal{A}_i^{\phi\phi} & 0 & 0 & 0 \\ 0 & 0 & \mathcal{A}_e^{cc} & 0 & 0 \\ 0 & 0 & 0 & \epsilon\mathcal{A}_e^{\phi\phi} & 0 \\ 0 & 0 & 0 & 0 & m_e \end{bmatrix}$$

In practice:

$$\epsilon^* \approx C_{\mathrm{diff}}/C_{\mathrm{adv}}$$

Conditioning with realistic parameter

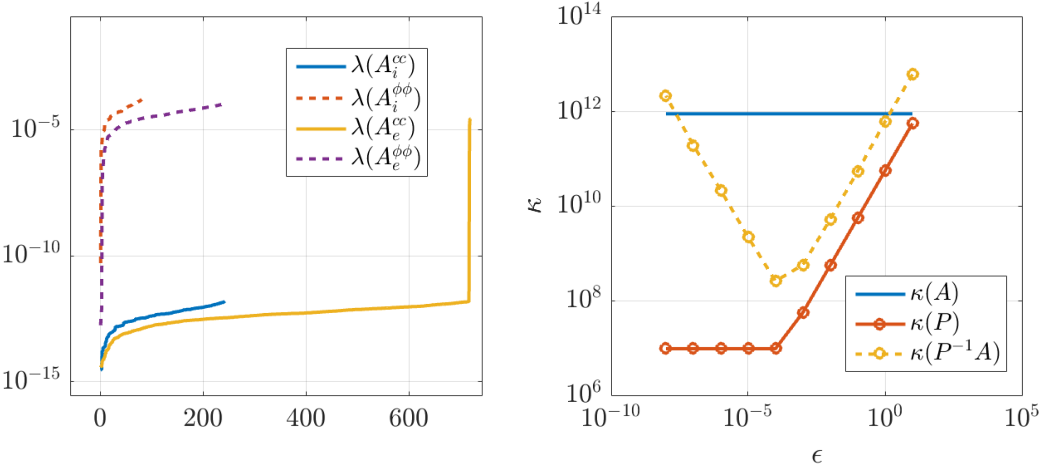

Numerical results: spatial robustness

(n, p)	$(32, 1)$	$(64, 1)$	$(128, 1)$	$(256, 1)$	$(512, 1)$
N	4612	17412	67588	266244	1056772
$\epsilon = 1$	89	89	58	53	28
$\epsilon = 10^{-1}$	10	10	10	10	10
$\epsilon = 10^{-2}$	7	7	7	7	7
$\epsilon = 10^{-3}$	7	7	7	7	7
$\epsilon = 10^{-4}$	5	5	5	5	5
$\epsilon = 10^{-5}$	7	18	36	21	26
$\epsilon = 10^{-6}$	28	28	30	36	24

(n, p)	$(16, 2)$	$(32, 2)$	$(64, 2)$	$(128, 2)$	$(256, 2)$
$\epsilon = 1$	90	85	59	59	29
$\epsilon = 10^{-1}$	10	10	10	10	10
$\epsilon = 10^{-2}$	7	7	7	7	7
$\epsilon = 10^{-3}$	7	7	7	7	7
$\epsilon = 10^{-4}$	5	5	5	5	5
$\epsilon = 10^{-5}$	7	7	15	11	36
$\epsilon = 10^{-6}$	36	25	36	36	12

Numerical results: time robustness and scaling

Δt	10^{-4} ms	10^{-3} ms	10^{-2} ms	10^{-1} ms	1 ms
Iterations	4	9	8	5	12